Reactive Molecular Dynamics Simulations for a Better Insight in Plasma Medicine

Annemie Bogaerts,* Maksudbek Yusupov, Jonas Van der Paal, Christof C. W. Verlackt, Erik C. Neyts

In this review paper, we present several examples of reactive molecular dynamics simulations, which contribute to a better understanding of the underlying mechanisms in plasma medicine on the atomic scale. This includes the interaction of important reactive oxygen plasma species with the outer cell wall of both gram-positive and gram-negative bacteria, and with lipids present in human skin. Moreover, as most biomolecules are surrounded by a liquid biofilm, the behavior of these plasma species in a liquid (water) layer is presented as well. Finally, a perspective for future atomic scale modeling studies is given, in the field of plasma medicine in general, and for cancer treatment in particular.

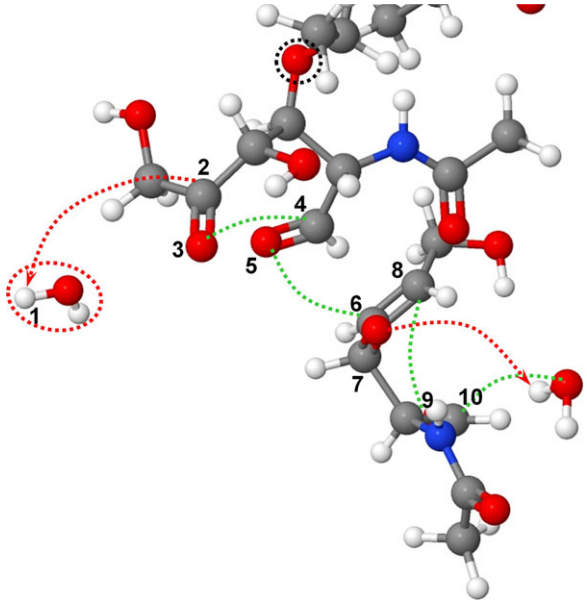

1. Introduction

Plasma medicine is a rapidly growing research field.[1–5] Nowadays it is one of the major topical research areas of low-temperature plasmas. The fields of application include disinfection of both living tissue and non-living surfaces (medical tools, diagnostic devices, etc.[6]), tooth bleaching,[7] treatment of skin diseases,[8] blood coagulation,[9] killing or apoptosis of cancer cells,[10–21] and even tissue regeneration.[22]

For improving these applications, a good insight in the interaction of the plasma with the relevant biomolecules is indispensable, in order to control the processes occurring in the contact region of the plasma with the bio-organisms. However, this still remains a big challenge. A number of fundamental investigations of the interaction of plasma species with specific biomolecules have already been carried out by experiments (e.g.,[23–26]). On the other hand, computer simulations may also be very valuable, and complementary to experiments, as they can study the interaction processes in detail, even on the atomic level, which is difficult to achieve by experiments. Nevertheless, so far not so many modeling efforts have been reported for studying the interaction processes between plasma species and biomolecules. A recent review highlighting the various simulation studies, including both atomic-scale methods (i.e., ab initio molecular dynamics (MD), reactive and non-reactive classical MD), and macroscale methods (typically as part of hydrodynamic models, that are used to describe the plasma behavior) was recently presented in ref.[27]

Macroscale methods (e.g.,[28–32]) typically make use of reaction–diffusion equations[28] or a reactive penetration model for mass-transfer of plasma species across a gas-liquid boundary.[29] Babaeva et al.[30–32] developed a model to describe the non-plasma material (such as skin tissue or individual cells) by considering it as a dielectric material with certain conductivity and permittivity, to represent for

A. Bogaerts, M. Yusupov, J. Van der Paal, C. C. W. Verlackt, E. C. Neyts
Research Group PLASMANT, Department of Chemistry, University of Antwerp, Universiteitsplein 1, B-2610, Wilrijk-Antwerp, Belgium
E-mail: annemie.bogaerts@uantwerpen.be

DOI: 10.1002/ppap.201400084

instance the cell membrane. Conservation equations were solved for both surface and volume charges on and inside the tissue material to obtain information on surface charging due to the impact of ions or electrons. Moreover, the Poisson equation yields the electric field distribution in the cellular structures. Typical results of such simulation studies include the fluxes and densities of photons, radicals and ions towards the treated surface. This type of model can yield information about plasma–tissue interaction in the millisecond time-scale and beyond, but due to the nature of these models, the resolution is limited to the supra-molecular level. This allows, for instance, to obtain some insight in the propagation of electric fields through a wound, but it cannot provide information on the atomic-scale interaction of plasma species with biomolecules. Furthermore, this type of models makes use of input parameters, such as the conductivity and permittivity of a cell, which are not always well known, so this modeling approach is more approximate.

In MD simulations, on the other hand, the interactions of plasma species with biomolecules are described on the atomic level, because the behavior of individual atoms is followed as a result of the forces acting upon them. These forces may either be obtained from quantum mechanical calculations (i.e., "ab initio MD") or be derived from a classical interatomic interaction potential or force field (i.e., "classical MD").

In the context of plasma medicine, all ab initio MD simulations are so-called Car-Parinello MD, based on density functional theory (DFT), and they have been applied for instance to investigate DNA damage caused by radicals.[33–35] This approach is very accurate, but it requires very long calculation times. Typically, only systems of around 100 atoms at the picosecond time-scale can be handled.[27]

Classical MD simulations are also quite time-consuming, but they can handle much larger systems, i.e., up to 10^3–10^5 atoms, at a time-scale of 10^2–10^5 ps, depending on the force field used.[27] Classical MD simulations can be subdivided into so-called reactive and non-reactive MD. In non-reactive MD simulations, the force field does not allow to simulate bond breaking or formation. For this reason, it can typically handle somewhat larger system sizes and time-scales, as the atomic connectivity does not have to be recalculated every time-step, but of course, it cannot be used to describe the chemical reactions of plasma species with biomolecules. It has typically been applied in literature for describing electroporation and ion transport through lipid bilayers (e.g.,[36,37]).

Therefore, when chemical reactions of plasma species with biomolecules are envisaged, reactive MD simulations are the method of choice. No assumptions need to be made with respect to the processes that are occurring, as they are self-consistent, and therefore ideally suited to study reaction mechanisms. They only require a suitable, accurate, and realistic interatomic interaction potential (or force field). As the forces on the atoms and thus the entire system dynamics depend on the latter, it is clear that this is the most crucial aspect of classical reactive MD simulations. There exist several reactive force fields in literature, but in the context of plasma medicine, only the Brenner potential[31] and the ReaxFF potential[38–43] have been applied.

Babaeva et al.[31] studied the sputtering processes of lipid-like material, and reported that prolonged exposure of this lipid-like film to energetic ions can produce significant carbon removal. Abolfath et al.[38] investigated the damage to a fragment of DNA in solution by free OH radicals, which are primary products of megavolt ionizing radiation in water-based systems. They found that OH radicals are the main source of H-abstraction and formation of carbonyl and hydroxyl groups, which finally results in DNA single and double strand breaks.

Recently, we have also performed a number of reactive MD simulations in our group for the interaction of important plasma species with several types of relevant biomolecules.[39–43] More specifically, we have studied the interaction of reactive oxygen species (ROS) with peptidoglycan, an important component of the outer cell wall of gram-positive bacteria,[39,40] and with lipid A, present in the cell wall of gram-negative bacteria,[41] as well as with lipids present in human skin.[42] Moreover, as most biomolecules are surrounded by a biofilm, we have also investigated the behavior of these plasma species in a liquid water layer (as simple model system for the biofilm), to elucidate which plasma species can effectively reach the biomolecules.[43] An overview of these modeling efforts, and some typical calculation results, will be presented in this paper. The simulations have not yet been applied to cancer cells, but the same methodology can (and will) be used in our future work for model systems relevant to cancer treatment, so the present examples also illustrate the possibilities in that respect. Finally, we will give a perspective of future opportunities and challenges for atomic-scale modeling of plasma–biomolecule interaction, for plasma medicine in general, but also more in particular for plasma oncology.

2. Computational Details

Classical (reactive) MD simulations are based on the time-integration of the equations of motion of all atoms in the system. The forces acting on these atoms are calculated as the negative derivative of a suitable (reactive) interatomic interaction potential. We make use of the ReaxFF potential, which was originally developed for hydrocarbons,[44] but later on expanded to a variety of other elements. It is

currently one of the most widely parametrized reactive force fields available, and it can describe nearly half of the periodic table of the elements and a wide variety of multi-element compounds. ReaxFF is capable of describing both covalent and ionic bonds, as well as the entire range of intermediate interactions. The ReaxFF parameters are optimized to obtain good general agreement with quantum mechanical calculations for structural energies, barriers, and structures (in that order of importance). It accurately simulates bond breaking and bond formation processes. It is known to be among the most accurate classical reactive force fields available, with an accuracy for hydrocarbons similar to or better than quantum-mechanical calculations at the PM3 level, while being 100 times faster.[44]

The ReaxFF parameters used for describing the interaction of ROS with peptidoglycan, with the lipids present in the skin and with the water layer are taken from the ReaxFF C/H/O/N glycine/water-force field, developed by Rahaman et al.[45] However, for describing the specific molecular system of lipid A, the force field should additionally contain parameters for P. A ReaxFF force field containing parameters for these atoms has been used in the work of Abolfath et al.[38]. However, this specific force field appeared not to be suitable for an accurate description of the lipid A system, as it was specifically designed to describe DNA and related molecules. To address this problem, two different force fields were combined, i.e., the parameters for the C/H/O/N elements were obtained from ref.,[45] whereas the P parameters were adopted from ref.[38]

Note that we limit ourselves to the interaction of ROS with these biomolecules and water, although reactive nitrogen species (RNS) are also found to have bactericidal effects. However, the currently available force fields do not accurately describe reactions of RNS with biomolecules. Also the force field parameters for O_3 are subject to uncertainties, so we do not focus on O_3 either. In the near future, we hope that a more accurate force field for RNS (and O_3) becomes available, so that we can also study the interaction processes of these species.

In the simulations, the biomolecular structure (see following sections) is typically placed in a box with dimensions in the order of several nm^3. Depending on the system, either fixed boundary conditions are applied (to prevent translation and geometric deformation of the structure; as in the case of peptidoglycan and lipid A; see Sections 3 and 4 below), or periodic boundary conditions in the x and y direction (i.e., to mimic an infinite surface, like for the interaction of plasma species with the lipid matrix in the skin or with the water layer; see Sections 5 and 6 below). Prior to the particle impacts, the structure is typically equilibrated at room temperature, using the Berendsen thermostat for the peptidoglycan simulations, and using the Bussi thermostat for all other simulations. The relaxation constant was set to 100 fs.

It should be realized that we have investigated the interaction of the plasma species with the biomolecular structures in the gas phase, i.e., not surrounded by a liquid film, in order to focus better on the chemical reactions with the real biomolecules (see Sections 3–5). However, in reality, the biomolecules are typically surrouned by a liquid film. We have also attempted some simulations of the interaction of plasma species with a biomolecule surrounded by a liquid film, but to avoid holes in the liquid film through which the plasma species could penetrate, we had to consider a large number of molecules in the simulation box, yielding a long calculation time. Therefore, in order to find out whether the plasma species can penetrate this liquid film and are able to reach the biomolecular structure, we have separately investigated the behavior of various plasma species in a liquid layer, as will be outlined in Section 6.

To describe the impacts of the plasma species, typically 10 incident particles (e.g., 10 OH radicals) are randomly positioned at a minimum distance of 10 Å around the biomolecular structure and also from each other. This distance ensures that there is initially no interaction between the plasma species and the biomolecule. The initial energy of the impinging plasma species corresponds to room temperature and their velocity directions are chosen randomly. To study all possible reaction mechanisms and to obtain statistically valid results for bond-breaking processes, a large number (typically 50–100) of runs are performed for each plasma species to be considered (see next sections for details). The time step for integrating the equations of motion is typically in the order of 0.1–0.25 fs. A few million time steps (iterations) are run, corresponding to a total simulation trajectory of around 300–500 ps per species. It was carefully checked that this time is long enough to observe most chemical reactions to occur, although some processes can occur on a longer time-scale, but these would be beyond reach of the MD time anyway.

3. Interaction of Plasma Species with Gram-Positive Bacteria

In gram-positive bacteria, like *Staphylococcus aureus*, the cell wall is (mostly) composed of peptidoglycan (PG) (see Figure 1). It forms a mesh-like layer and serves as a protective barrier for bacteria. It is also present in gram-negative bacteria, but in that case, it is encapsulated by another membrane, composed among others of lipopolysaccharide (LPS); see Section 4 below. The PG layer is substantially thicker in gram-positive bacteria than in gram-negative bacteria. For instance, in the gram-positive

DOI: 10.1002/ppap.201400084

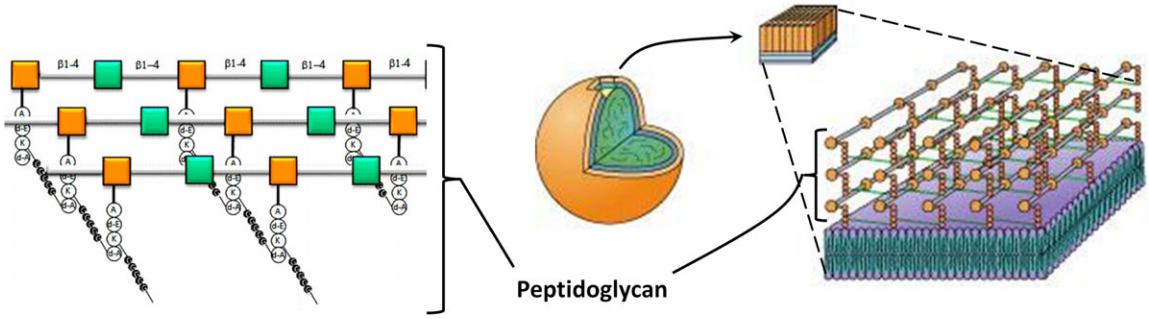

Figure 1. Schematic representation of the cell wall of gram-positive bacteria, and of peptidoglycan, as part of the cell wall.

bacterium *S. aureus*, the PG structure is typically 20–30 nm thick, whereas in a gram-negative bacterium, such as *Escherichia coli*, it is only 6–7 nm thick.[46] As PG is the outer protective barrier in gram-positive bacteria, it can directly interact with plasma species. If the latter can dissociate the important bonds in PG, this will lead to the destruction of the PG structure, and therefore result in structural damage of the bacterial cell wall.

PG is assembled from repeating units consisting of disaccharides (see Figure 1: orange and green squares), a stem (open circles in Figure 1) and a bridge (small solid circles in Figure 1). A detailed atomic-scale picture of the PG structure, as used in our simulations, is presented in Figure 2. The box size was set to 75 Å × 88 Å × 51 Å. The PG structure can be considered as a repeating unit, which includes all possible atomic bonds. It consists of two disaccharides (top left and bottom right in Figure 2), which are composed of β(1–4) linked *N*-acetylglucosamine and *N*-acetylmuramic acid (GlcNAc-MurNAc). The stem is in our case a tetrapeptide. Indeed, in the nascent PG, a pentapeptide L-alanine-D-*iso*-glutamine-L-lysine-D-alanine-D-alanine (L-Ala_1-D-*iso*-Gln_2-L-Lys_3-D-Ala_4-D-Ala_5) is found, but the last (fifth) D-Ala_5 residue is lost in the mature macromolecule.[47] Finally, the bridge (Figure 2: center) is a pentaglycine (Gly_1-Gly_2-Gly_3-Gly_4-Gly_5) interpeptide, branching off the ε-amino group of the L-Lys of the stem peptide, hence connecting one PG chain to the D-Ala_4 of a neighboring chain (see Figure 2).

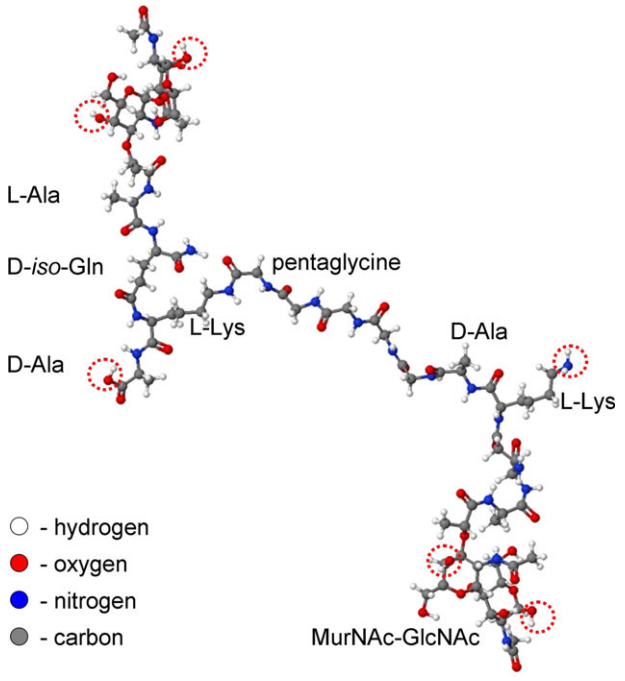

Figure 2. Atomic-scale representation of one repeating unit of the peptidoglycan structure. The red dash circles indicate the fixed atoms in the structure. (Reprinted from ref.[39] with permission from Institute of Physics).

We have investigated the interaction of the following ROS with PG: O, OH, O_2, O_3, H_2O, and H_2O_2.[39,40] As our later calculations[43] suggested that the force field used might not be accurate enough for describing the behavior of the O_3 molecules, we do not focus on this species in the present paper. Our calculations predict that O_2 and H_2O molecules cannot structurally damage the PG structure, but only interact with PG through hydrogen bridge formation. The other plasma species, i.e., O, OH, and H_2O_2, can break structurally important bonds of PG (i.e., C—O, C—C or C—N bonds), suggesting that they can yield the destruction of the bacterial cell wall. Table 1 illustrates the calculated fraction of important C—N, C—O, and C—C bond dissociations upon impact of O, OH, and H_2O_2.[40] It is clear that the OH radicals and especially the O atoms are more effective in bond cleavage than the H_2O_2 molecules, which is in correlation with experiments demonstrating the crucial role of O and OH in bacterial inactivation.[48–51]

Furthermore, our calculations reveal that the ether C—O bonds in the disaccharides break up more easily, followed by the C—C and C—N bonds in PG. In the case of H_2O_2 molecules, no C—N bond-breaking events were observed, indicating again that the H_2O_2 molecules might be somewhat less effective in bacterial cell wall destruction.

Table 1. Fraction of important C—N, C—O, and C—C bond breakings, and associated standard deviations, calculated from 50 independent simulations, upon impact of O, O_3, OH, and H_2O_2 on peptidoglycan. Note that the sum should not be 100%, as one species can lead to several (consecutive) bond breakings.

Incident plasma species	Fraction C—N bond breaking (%)	Fraction C—O bond breaking (%)	Fraction C—C bond breaking (%)
O atoms	26 ± 6	78 ± 6	38 ± 7
OH radicals	8 ± 4	54 ± 7	14 ± 5
H_2O_2 molecules	0	44 ± 7	12 ± 5

However, compared to the highly reactive O radicals, H_2O_2 molecules are stable species in an aqueous environment (see Section 6 below), and are thus more likely to reach the PG. Hence, it is expected that the H_2O_2 molecules are also very important for bacterial deactivation.

We have studied in detail the mechanisms of the important ROS-induced bond-breaking processes in PG. It was found that in all bond cleavage events the dissociation is initiated by H abstraction. However, a clear difference was observed in the mechanisms upon impact of H_2O_2 molecules on one hand, and OH and O on the other hand. Indeed, in the latter case the plasma species (OH or O) abstract an H atom from the PG, whereas in the case of H_2O_2 impacts, these molecules first react with each other, forming HO_2 radicals, from which an H atom is abstracted by an O atom in the PG structure. This can then cause the dissociation of the important bonds in PG. This correlates to the experimental observation that hydroperoxyl (HO_2) radicals are strong bactericidal oxidants and can cause the inactivation of bacteria in an aqueous environment.[52]

The structurally important C—O bonds are found both in the disaccharides (MurNAc–GlcNAc) as well as between them. Several C—O bond-breaking mechanisms were observed in our simulations, but as mentioned above, they are always initiated by H abstraction. In most cases, this leads to a cascade of C—O bond cleavage events, i.e., the breaking of three important C—O (ether) bonds: one in MurNAc, one in GlcNAc and one between them. One of the observed consecutive breaking mechanisms of three ether bonds is presented in Figure 3.[39] This example is for the impact of O atoms, but the same mechanism was also the most frequently observed one for all other impinging species.[39,40]

In Figure 3a, a first O atom abstracts an H atom from GlcNAc with the formation of an OH radical (see red dashed arrow and circle). After a few ps, another H atom is abstracted from MurNAc by a second O atom, yielding the formation of an OH radical (see Figure 3b: red dashed circle). This OH radical abstracts another H atom, connected to C_1, and a H_2O molecule is formed (see Figure 3c: red dashed circle). Consequently, a radical is created at C_1, which results in a cascade of homolytic C—O ether bond dissociations and double C=O and C=C bond formations. For clarity, the atoms that participate in the dissociation of the ether bonds are numbered (see Figure 3a: black dashed circles; and cf. the difference in bonds between the numbered atoms from Figures 3b and c). This cascade starts with the creation of a double $C_1{=}O_2$ bond, which in turn leads to the dissociation of the $C_3{-}O_2$ bond. The latter leads to the creation of a double $C_3{=}O_4$ bond, and the dissociation of the $C_5{-}O_4$ bond, which in turn yields the formation of a double $C_5{=}C_6$ bond. This finally results in the breaking of the $C_6{-}O_7$ bond and the creation of a double $C_8{=}O_7$ bond. Hence, this cascade process leads to cleavage of part of the molecule, which will probably result in damage to the bacterial cell wall.

As far as the C—C and C—N bonds are concerned, the cleavage of the C—C bonds occurs only in the disaccharides and in most cases after the breaking of three ether bonds. Finally, the C—N bond dissociations were found to occur most often in alanine, rather than in other parts of the

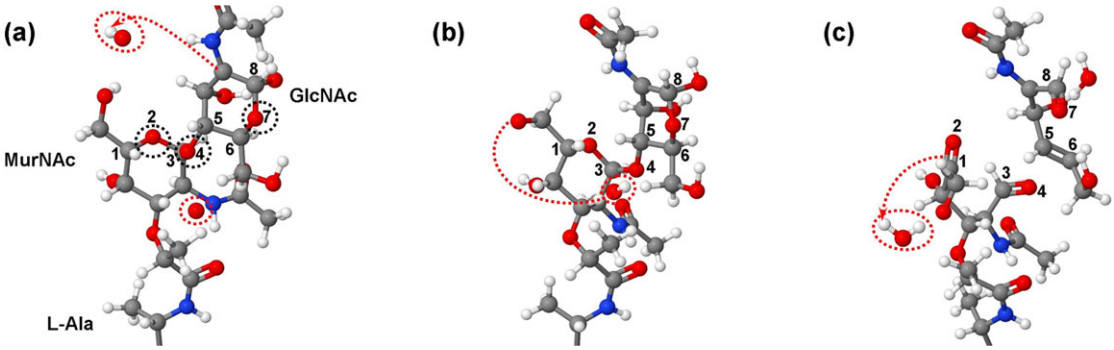

Figure 3. Snapshots from MD simulations, showing the consecutive dissociation of three (ether) C—O bonds (black dashed circles in (a)) upon O atom impact on peptidoglycan. The color legend is the same as in Figure 2. See text for explanation. (Reprinted from ref.[39] with permission from Institute of Physics).

DOI: 10.1002/ppap.201400084

PG structure. A more elaborate discussion of the interaction mechanisms between plasma species and PG can be found in ref.[39,40]

4. Interaction of Plasma Species with Gram-Negative Bacteria

As mentioned in Section 3 above, a PG layer is also present in gram-negative bacteria, but in this case it is encapsulated by an outer membrane, composed of an asymmetric bilayer. The outer leaflet of the outer membrane is composed of LPS, which consists of three parts, i.e., the outer O-antigen polysaccharide, the core oligosaccharide, and the inner hydrophobic lipid A (see Figure 4). The O-antigen is a repetitive hydrophilic glycan polymer of which the composition varies in different gram-negative bacteria. Since the O-antigen comprises the outermost region of gram-negative bacteria, it is targeted by hosts for antibody recognition. The O-antigen and core oligosaccharide serve to protect the bacteria, by keeping the structural integrity, whereas lipid A is the toxic part of the LPS.[25] It consists of multiple fatty acid chains connected to two glucosamine units containing a phosphate group.

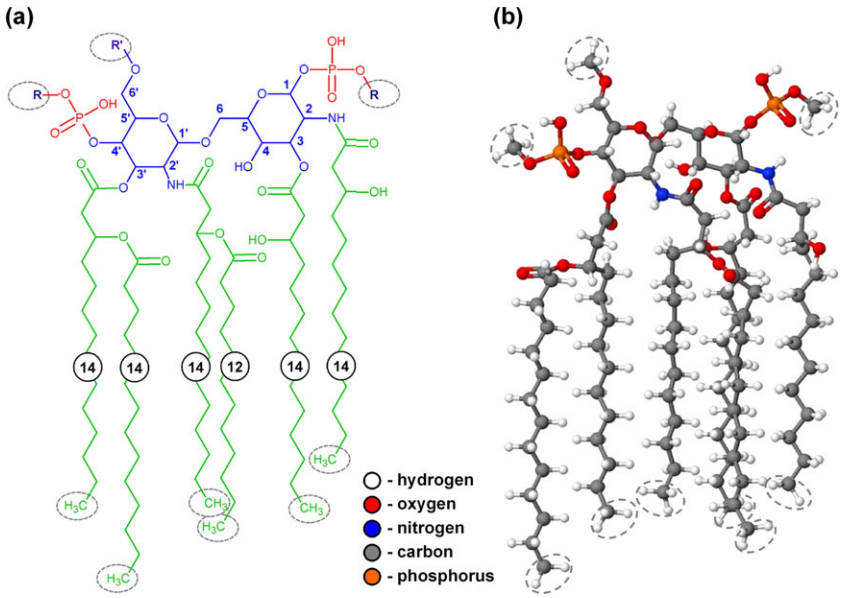

Figure 5. Atomic-scale representation of one repeating unit of the lipid A structure. The disaccharide backbone, phosphoryl part and aliphatic chains are indicated in (a) by blue, red and green colors, respectively. The repeating parts of the lipid A and the part connected to the oligosaccharide of LPS are denoted in (a) by R and R′, respectively. In our model structure (b), they are substituted by methyl residues. The number of carbon atoms in the aliphatic chains is indicated in black in (a). The gray dashed circles in both (a) and (b) indicate the fixed H atoms.

As we are mainly interested in the toxic part of the LPS, and in order to perform the simulations in a computationally efficient way, we focus only on lipid A, while the other parts of the LPS are simply substituted by methyl residues. An atomic-scale picture of the lipid A structure in *E. coli* is presented in Figure 5. The box size has dimensions of 50 Å × 70 Å × 40 Å. The lipid A structure consists of a β(1–6) linked D-glucosamine disaccharide (blue color in Figure 5a) carrying two phosphoryl groups at positions 1 and 4′ (red color in Figure 5a) and connected to fatty acids, ester-linked at positions 3 and 3′, and amide-linked at positions 2 and 2′ (green color in Figure 5a). These chains are then further connected to other fatty acids. In total there are six aliphatic chains, which are made up of 12–14-carbon chains (indicated in black in Figure 5a). The repeating parts of the lipid A and the part connected to the oligosaccharide (which are specified with R and R′, respectively; see Figure 5a) are replaced by methyl residues (cf. Figure 5b).

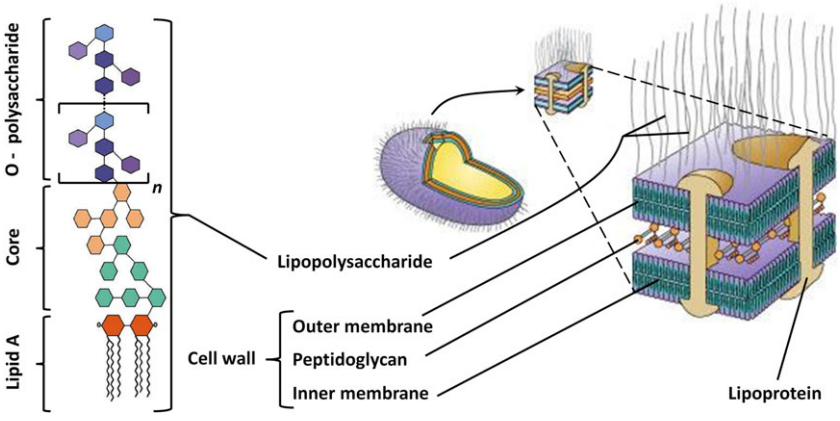

Figure 4. Schematic representation of the cell wall of gram-negative bacteria, and of lipopolysaccharide, as part of the cell wall.

The toxic activity of lipid A is highly correlated to its molecular structure. Any deviation from its structure (e.g., the number and length of the fatty acid groups, as well as the phosphorylation state) decreases the toxicity of lipid A.[53] Thus, studying the interaction of plasma species with lipid A will improve our understanding about the destruction mechanisms of lipid A molecules, and will give us a better insight in the antibacterial properties of plasmas.

We have studied the interaction of OH, HO_2, and H_2O_2 with the lipid A structure

shown in Figure 5. These plasma species can indeed destroy the lipid A structure, resulting in a drop of its toxicity. Similar to PG (see Section 3 above), the interaction mechanisms are always initiated by H abstraction reactions. In the case of HO_2 and H_2O_2, the H atom is typically abstracted from the impinging particle itself, whereas in the case of OH radicals, it is abstracted from the lipid A structure. We observed the destruction of the hydrophilic head (i.e., the disaccharide and phosphoryl groups) upon impact of these different species, whereas the destruction of the aliphatic chains occurred mainly upon impact of the OH radicals.

Figure 6 illustrates the destruction of the hydrophilic head upon impact of an OH radical. First, an H atom is abstracted (see black dashed circle in Figure 6), leading to the formation of a water molecule. This subsequently results in the consecutive breaking of three C—O bonds (see gray dashed lines), and the formation of two double C═O bonds and one double C═C bond. Besides the destruction of the disaccharide part, also the phosphate group is detached, as is clear from Figure 6. This indicates that the plasma species can indeed decrease the toxic character of the lipid A, as lipid A with a single phosphoryl group is known to be 1 000-fold less active than the lipid A with two phosphoryl groups in *E. coli*.[53]

The damage of the aliphatic chain upon impact of OH radicals is illustrated in Figure 7. An H atom positioned close to the ester is abstracted (see black dashed circle), yielding the formation of a water molecule. This H abstraction leads to the formation of a double C═C bond and the cleavage of a C—O bond (see gray dashed line), hence the detachment of an aliphatic chain. Note that the number of aliphatic chains has also a direct effect on the toxicity of lipid A, as a structure with six fatty acid groups expresses the optimal endotoxic activity.[54] Note that the desorption of the aliphatic chains is only observed in a limited number of cases upon impact of HO_2 and H_2O_2. More details about the interaction mechanisms of the ROS with lipid A can be found in ref.[41]

The obtained results are in good qualitative agreement with experimental observations.[24–26] Indeed, Bartis et al.[24] reported a drop in C—C and C—H signals in XPS

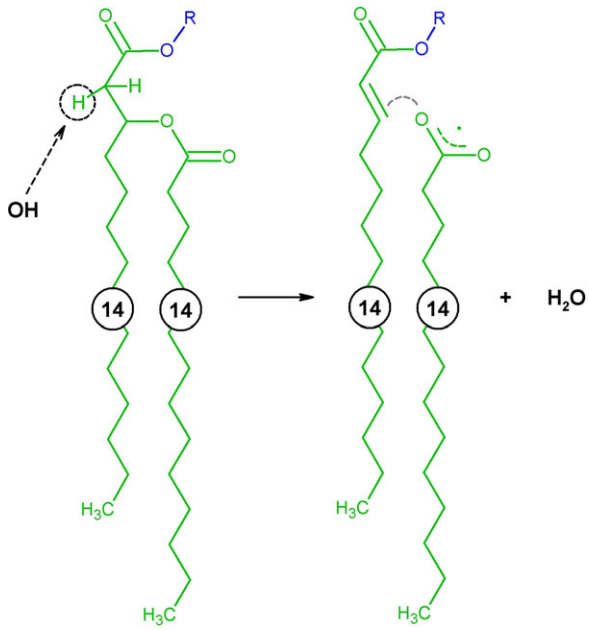

Figure 7. C—O bond breaking mechanism in one of the aliphatic chains of lipid A (green color; see Figure 5(a)) upon H abstraction by an incoming OH radical. For the sake of clarity, the disaccharide part is substituted in this figure with R (blue color). See text for explanation.

and a slight drop in the O—C—O, N—C═O and O—C═O signals, while the C—O and C═O signals increased when treating LPS with ROS. The drop in C—H bonds can be correlated with the H abstractions upon OH impact, while the drop in C—C bonds is related to the formation of double C═C bonds in our simulations. Also, the breaking of O—C—O bonds (see Figure 6) and the detachment of aliphatic chains (i.e., breaking of O—C═O groups; see Figure 7) is in agreement with the XPS measurements.[24] Moreover, this bond breaking leads to the formation of double C═O bonds, which was also observed experimentally.[24] Finally, the increase in C—O groups is also predicted by our simulations, at least for the OH radical impacts, and is attributed to the creation of new OH groups in the aliphatic chains. Furthermore, Chung et al.[25]

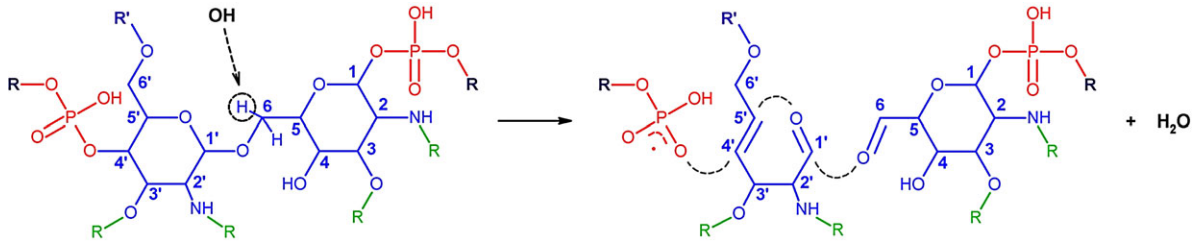

Figure 6. Breaking mechanism of three C—O bonds in the disaccharide part of lipid A (blue color; see Figure 5(a)) upon H abstraction by an incoming OH radical. For the sake of clarity, the aliphatic chains are substituted in this figure with R (green color). See text for explanation.

DOI: 10.1002/ppap.201400084

reported that the phosphate moieties and intact aliphatic chains all drop significantly upon O radical impact, which agrees with our simulation results for OH radical impacts. Note that we have also performed test simulations for O radicals, and the same mechanisms were observed as for the OH radicals. However, as the O radicals cannot penetrate the liquid layer (see section 6 below), we did not focus on these species here. Finally, Bartis et al.[26] reported that the radical treatment did not significantly affect the phosphorous and nitrogen content, in contrast to direct and UV/VUV treatments of LPS, which is consistent with our simulations, as we did not observe bond-breaking events in the phosphoryl groups (i.e., no P—O bonds were broken) as well as negligible breaking of the C—N bonds.

5. Interaction of Plasma Species with Lipids in the Skin

We have also performed simulations for the interaction of ROS with lipids present in the upper part of the skin layer, or stratum corneum. The lipid matrix present in the stratum corneum is composed of fatty acids, ceramides and cholesterol.[8,55] In first instance, we have performed simulations of the interaction of O and OH radicals with α-linolenic acid, which is assumed to be representative for the fatty acids present in the stratum corneum, as it has a typical chain length and a typical number of double bonds. The box size in these simulations was set to 20 Å × 20 Å × 40 Å. Several mechanisms were observed to occur, such as the formation of a conjugated double bond, and the insertion of alcohol and aldehyde functional groups.[42] Again, these processes are mostly initiated by H abstraction.

Figure 8 illustrates the mechanism for the formation of an alcohol and subsequently an aldehyde upon impact of 3 O radicals. The same process can also happen upon impact of other H-abstracting species. After a first H abstraction (see A and B in Figure 8), resulting in the formation of an OH radical, this OH radical attaches to the formed alkyl radical site (Figure 8B and C), leading to the formation of an alcohol (Figure 8C). Upon impact of two more O radicals (or other H-abstracting species), the H atom from this alcohol group as well as an H atom from the adjacent C atom can also be abstracted (green circle in (Figure 8B) and blue circle in (Figure 8D), respectively). This yields the formation of a double C═O bond, hence creating an aldehyde group (Figure 8E). The corresponding reaction scheme is also illustrated in Figure 8.

The insertion of these functional groups will increase the hydrophilic character of the skin layer and it will change the lipid composition of the skin, and this might have consequences for the underlying tissue. The observed reactions are in qualitative agreement with experiments,[8] where a rise in the number of C—O and C═O bonds, attributed to alcohol and aldehyde groups, as well as a

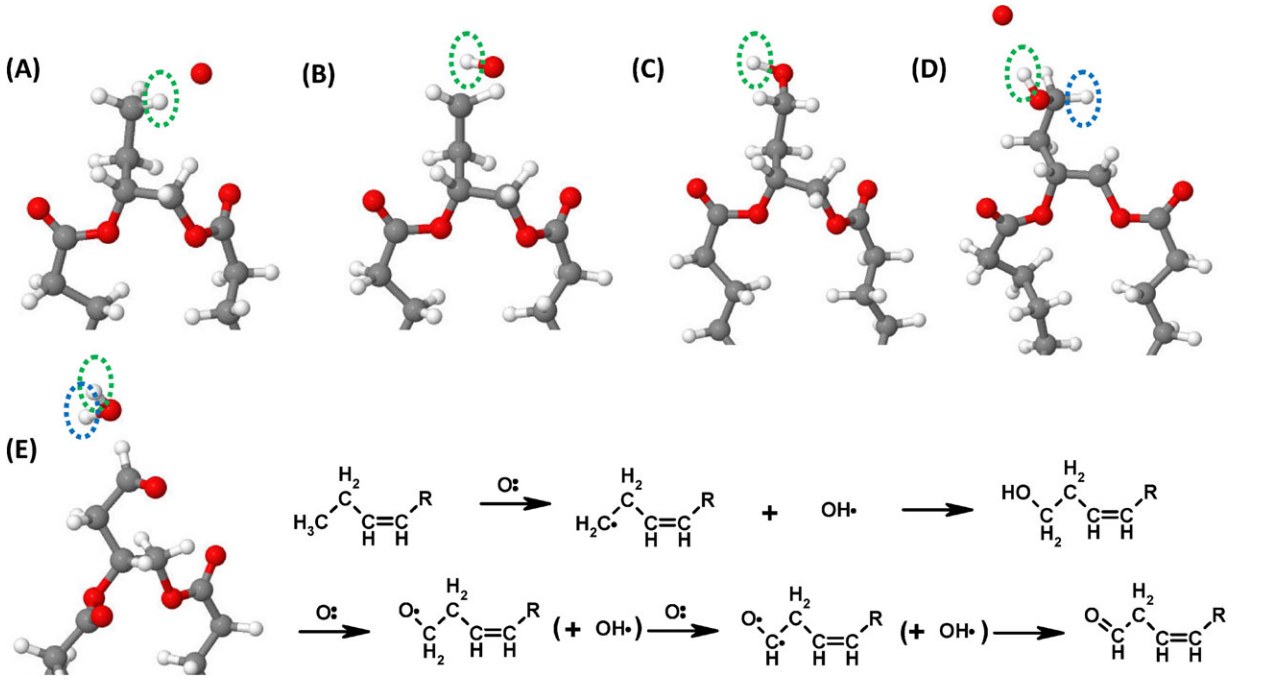

Figure 8. Snapshots from MD simulations, and corresponding reaction scheme, showing the formation of an alcohol group and subsequently an aldehyde group upon three subsequent impacts of O radicals on one α-linolenic acid molecule. See text for explanation. (Reprinted from [42] with permission from Institute of Physics).

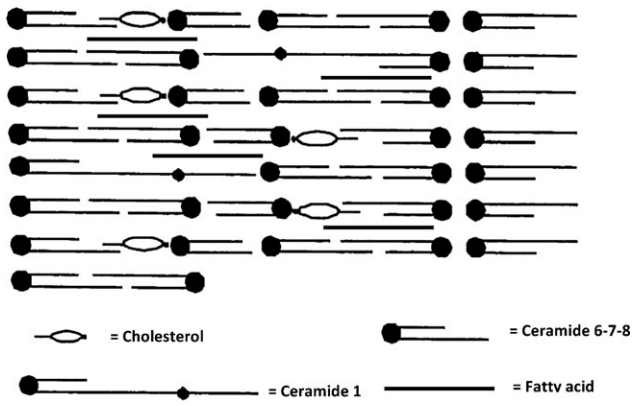

Figure 9. Schematic diagram of the model system for the lipid matrix in the stratum corneum, composed of fatty acids, ceramides, and cholesterol.

general rise in the O-content, was reported in the tissue after treatment with a plasma. On the other hand, it should also be mentioned that no toxic lipid peroxidation products were formed in our simulations, which might be attributed to limitations in the force field, or to the limited time-scale of the MD simulations.

Recently, we have extended this study to a more realistic model system, composed of free fatty acids, ceramides, and cholesterol, as schematically illustrated in Figure 9. The ceramides present in the stratum corneum are ceramide 1, 6, 7, and 8, with relative concentrations of 11, 33, 22, and 33%, respectively.[56] The chemical structures of these ceramides are depicted in Figure 10, together with the actual simulation box used for this study. Periodic boundaries are used in the *x*- and *y*-directions, while the ROS impinge the structure from above (*z*-direction).

Our simulations indicate that again various mechanisms occur, again mostly initiated by H abstraction. The most common process is the break-up of the ceramides, although oxidation of an alcohol group and formaldehyde formation occur as well. The mechanism of ceramide break-up upon impact of 2 OH radicals is schematically illustrated in Figure 11 for ceramide 7 (depicted at the left part), including some snapshots of the MD simulations (upper part), as well as the reaction scheme (lower part). The OH radicals abstract 2 H atoms from an alcohol group, yielding the formation of a water molecule (MD snapshots A–C; and indicated with blue and green dashed circles in both the MD snapshots and the reaction scheme). Subsequently, a C—C bond breaks, and two aldehydes are formed (MD snapshot D; and indicated with the red dashed circles in both the MD snapshots and the reaction scheme). These simulations suggest that the lipid layer loses its structure due to the break-up of the ceramides, so that radicals, as well as other molecules (such as drugs) might be able to penetrate deeper in the lipid structure. This is in qualitative correspondence with observations from literature.[57]

6. Behavior of Plasma Species in a Liquid Film Surrounding Biomolecules

It should be realized that the MD simulations outlined above, all correspond to "ideal" conditions, because in reality, biomolecular structures such as bacteria are typically surrounded by a liquid film; hence, the plasma species first need to penetrate this liquid film before they can interact with the biomolecules. Therefore, we have also investigated the behavior of various ROS (i.e., O, OH, HO_2 radicals and H_2O_2 molecules) in a liquid film, using pure water as a starting point, i.e., as the most simple model system.[43]

The interaction of O and subsequently OH radicals with the H_2O molecules is illustrated in Figure 12. The O atoms react with a H_2O molecule, forming two OH radicals (Figure 12a–c). Hence, the O radical is lost and the OH radicals can now interact with the H_2O molecule, with the formation of new OH radicals, as shown in (Figure 12d–f). The HO_2 radicals (not shown) also react with the H_2O molecules, yielding O_2^- and H_3O^+ ions, but the reverse reaction occurs within a few fs, so that new HO_2 radicals are formed. Finally, the H_2O_2 molecules were

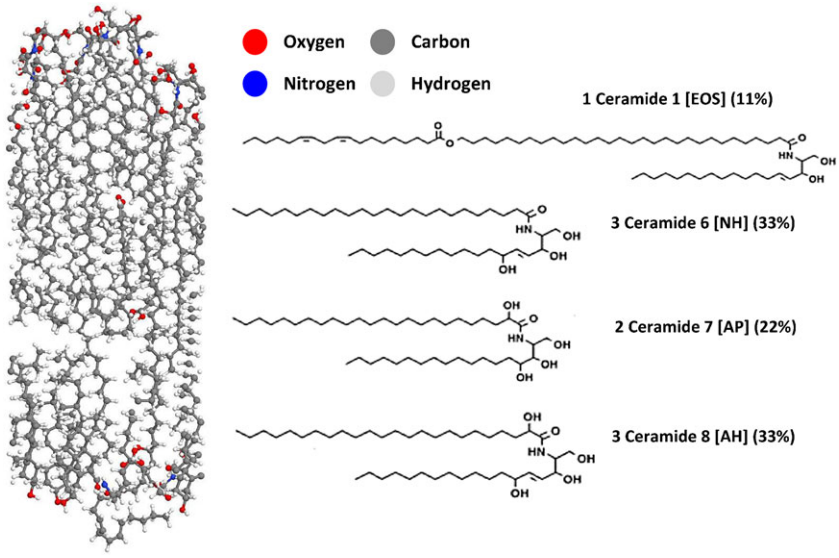

Figure 10. Simulation box of the lipid matrix, consisting of free fatty acids, ceramides and cholesterol. The various ceramides included in this lipid maxtrix are depicted at the right, with their name and relative concentration.

DOI: 10.1002/ppap.201400084

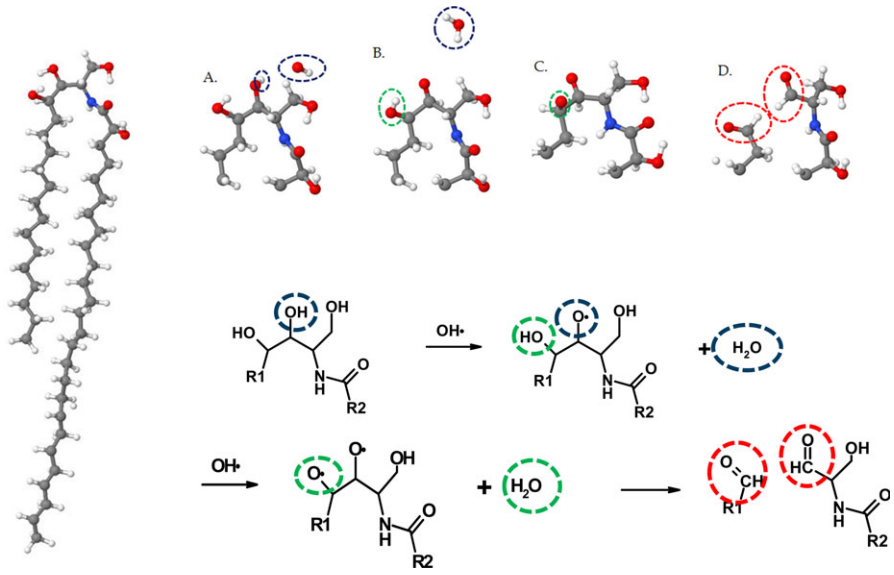

Figure 11. Break-up mechanism of ceramide 7 (see left part), upon impact of two OH radicals, including snapshots of the MD simulations (upper part) and reaction scheme (lower part). See text for explanation.

found not to react with the H_2O molecules. Summarized, our simulations predict that the O atoms cannot travel through the water layer, but the OH, HO_2, and H_2O_2 molecules can (either without reacting, such as H_2O_2, or with reacting but forming the same species again, like OH and HO_2), and can most probably reach the bio-organisms. They also form some other species, so the most important (i.e., first and second generation) plasma species that will be

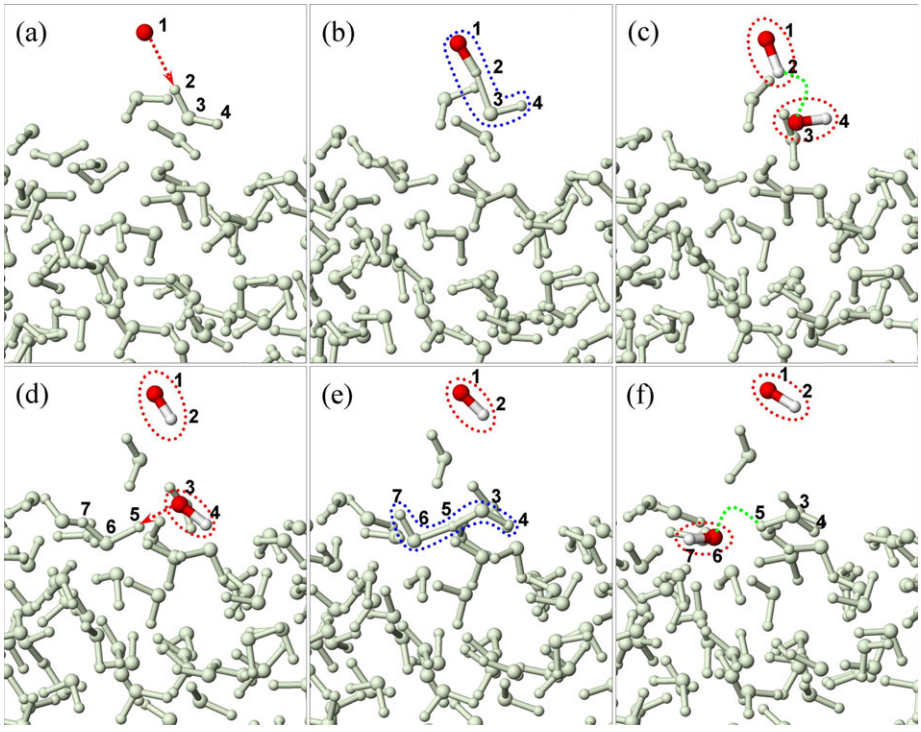

Figure 12. Snapshots from MD simulations, showing the interaction of an O atom with water, resulting in the formation of two OH radicals (a–c), which subsequently react with water (d–f). The water molecules are illustrated in grayish green color. The reaction intermediates are shown within blue dashed closed-curves. The newly formed OH radicals are presented in red dashed circles. The cleavage of bonds is indicated by green dashed lines. (Reprinted from ref.[43] with permission from Institute of Physics).

present in the liquid layer, and can possibly interact with the bio-organisms, as predicted by our simulations, are OH, HO_2, O_2, O_2^-, H_3O^+ and H_2O_2. More information about the behavior of these ROS in the water layer, including their trajectories and the estimated diffusion coefficients, can be found in ref.[43]

7. Conclusion and Perspective

We have presented some characteristic results of reactive MD simulations for the interactions of ROS from the plasma with biomolecules, to illustrate the potential of this type of simulations. The examples presented include the interaction with (i) peptidoglycan, as part of the cell wall of gram-positive bacteria, (ii) lipid A, present in the cell wall of gram-negative bacteria, and (iii) a lipid matrix present in the outer skin layer (stratum corneum), as well as (iv) the behavior of these ROS in a liquid (water) layer, which is typically surrounding the bio-organisms.

Our simulations predict that O_2 and H_2O molecules do not chemically react with the bio-organisms, whereas O, OH, HO_2 radicals and H_2O_2 molecules do react, and can give rise to the destruction of the bio-molecules. In the case of peptidoglycan and lipid A, this might result in killing of the bacteria, or at least decreasing their toxicity. In the case of the lipid matrix of the stratum corneum, we found that functional groups (i.e., alcohol and aldehyde groups) can be inserted in fatty acids, thereby increasing the hydrophilic character of the skin layer, which might have consequences for the underlying tissue. Furthermore, the ROS can break up the ceramides present in the lipid matrix, so that the latter might lose its structure. As a consequence, radicals and other molecules (such as drugs) might be able to penetrate deeper in the lipid structure of the skin. Finally, from the behavior of the ROS in a liquid water box, we can conclude that O atoms cannot travel through the water layer, as they immediately form OH radicals, whereas the OH, HO_2 radicals and H_2O_2 molecules can penetrate and can most probably reach the bio-organisms. In the future, we plan to include other components in the water layer, which are known to be present in a biofilm, such as proteins, sugars, and other hydrocarbons.

These examples demonstrate the potential of reactive MD simulations, but also illustrate some of their inherent limitations. First, they are subject to long calculation times, i.e., in the order of several weeks on today's fast computers, for the examples shown here. Therefore, they are inherently limited to (relatively) small systems, in the order of 10 000 atoms, or a simulation box of a few nm^3 (although it should be realized that this is much larger than ab initio type simulations[27]). This means that it is not possible to simulate, for instance, an entire cell. A possible solution could be to use a combination of reactive MD with non-reactive MD simulations. The latter are computationally less intensive, and can therefore handle larger systems (i.e., in the order of 100 s of nm[27]). However, they do not capture the breaking and formation of bonds, so they cannot describe the chemical reactions of plasma species with biomolecules. By using a combination of non-reactive MD, for predicting the structure of the larger framework, and reactive MD, for describing the chemical reactions at the biochemically most interesting parts of the structure, larger systems can possibly be handled. Furthermore, it would be even more interesting, and relevant for the applications, if these atomic-scale simulations could be coupled to macroscale simulations, like e.g., presented in ref.,[28–32] by using detailed atomistic MD results (e.g., chemical reaction probabilities) as input for macroscale simulations, to cover a much wider scale of the biomedical systems.

Second, again because of the long calculation times, the dynamical system evolution can only be described for short time-scales, i.e., in the order of a few ns or perhaps a few tens of ns at maximum. Hence, processes occurring on much longer time-scales (e.g., diffusion of transmembrane proteins in the cell membrane, healing of electroporated cell membranes, vesicle formation, apoptosis and other global processes) will not be captured by the MD simulations. There exist several techniques to extend the time-scale, e.g., parallel replica, hyperdynamics and temperature-accelerated dynamics, with a so-called "boost factor" in the order of $10–10^7$, at least when the system obeys transition state theory and when the barriers to be crossed are high compared to kT.[58] This condition would be satisfied at low temperatures and on well-defined systems, such as single crystals, but not necessarily on biomolecules. Another speed-up method is coupling MD simulations with Monte Carlo (MC) techniques.[59–61] Our group has already demonstrated that the so-called force bias MC (fbMC) methodology[59,60] is very suitable for simulating the growth of nearly defect-free carbon nanotubes with specific chiralities, which is not possible with pure MD simulations, and which is attributed to relaxation processes, that are indeed occurring on longer time-scales.[62,63] When the MD simulations can be combined with the above-mentioned acceleration methods, we might be able to also capture processes that happen on longer time-scales in the interaction of plasma species with biomolecules.

Finally, it is of utmost importance to realize that the results obtained by MD simulations depend crucially on the accuracy of the force field used. The ReaxFF force field employed in our work is probably the most generic classical force field currently available, and it is stated to be comparable in accuracy to semi-empirical quantum chemistry calculations, while being 100 times faster.[44] Nevertheless, the force field currently used in our simulations cannot yet describe chemical reactions of RNS with

DOI: 10.1002/ppap.201400084

biomolecules in an accurate way. Moreover, we experienced that this force field did not yet accurately describe reactions of O_3 molecules with water.[43] It is thus clear that one should always use and apply available force fields with some caution.

In our future work, we wish to extend our MD research to the field of plasma oncology. It is clear that plasmas have beneficial effects for cancer treatment, but the underlying mechanisms, e.g., of plasma-induced apoptosis, are not yet fully understood.[14–16] It will for sure be interesting to study the interaction of ROS (which might be generated inside the cell by plasma species) with DNA, causing irreversable damage (i.e., double strand break) leading to controlled (apoptosis) or uncontrolled (necrosis) cell death.[17–19] Moreover, as cancer cells seem to be able to escape from the immune system,[64,65] which is recently described as a hallmark for cancer,[66] it might also be of interest to study the interaction of plasma species with (parts of) immunocells, to investigate whether the plasma can stimulate the immune system.[67] Furthermore, the interaction of plasma species with the mitochondrial outer membrane will probably be very relevant, because changes in the mitochondrial outer membrane permeability stimulate the release of pro-apoptotic agents.[18,20] Last but not least, also the interaction of plasma species with the eukaryotic cell membrane will be of great interest, as this might lead to cell detachment by breaking the cell adhesion molecules,[15] or to find out whether the plasma species can penetrate the cell membrane and form intracellular ROS or lipid peroxidation products,[17,19,21] which will increase the membrane permeability and cause damage to the membrane proteins, until the cell membrane collapses and the cell is damaged. Likewise, the influence of the electric field and of ions originating from the plasma on cell membrane permeabilization will be interesting to study. For this purpose, a combination of non-reactive MD (for studying electroporation) and reactive MD (for studying the chemical reactions of the relevant plasma species with the membrane lipids) might be very useful.

In conclusion, we can identify many different aspects of cancer at the molecular/cellular level, that might be interesting to study with reactive MD simulations. The main challenge, besides the availability of accurate force fields that can handle all atoms of interest (cf. above), will be to define suitable model systems, which are large enough to be relevant, and small enough to be handled within a reasonable calculation time.

Acknowledgments: This work was financially supported by the Fund for Scientific Research Flanders (FWO). The authors would like to thank A. C. T. van Duin for sharing his ReaxFF code for our simulations. The calculations were carried out in part using the Turing HPC Infrastructure of the CalcUA core facility of the Universiteit Antwerpen, a division of the Flemish Supercomputer Center VSC, funded by the Hercules Foundation, the Flemish Government (department EWI) and the Universiteit Antwerpen.

Received: May 17, 2014; Revised: July 26, 2014; Accepted: August 18, 2014; DOI: 10.1002/ppap.201400084

Keywords: bacteria; biomolecules; molecular dynamics simulations; plasma medicine; reactive oxygen species

[1] M. G. Kong, G. Kroesen, G. Morfill, T. Nosenko, T. Shimizu, J. van Dijk, J. L. Zimmermann, *New J. Phys.* **2009**, *11*, 115012.
[2] K. Ostrikov, E. C. Neyts, M. Meyyappan, *Adv. Phys.* **2013**, *62*, 113.
[3] M. Yousfi, N. Merbahi, A. Pathak, O. Eichwald, *Fundam. Clin. Pharmacol.* **2014**, *28*, 123.
[4] M. Laroussi, M. G. Kong, G. E. Morfill, W. Stolz, *Plasma Medicin : Applications of Low-Temperature Gas Plasmas in Medicine and Biology*, Cambridge University Press, Cambridge **2012**.
[5] T. von Woedtke, S. Reuter, K. Masur, K.-D. Weltmann, *Phys. Rep.* **2013**, *530*, 291.
[6] Y.-F. Li, T. Shimizu, J. L. Zimmermann, G. E. Morfill, *Plasma Process. Polym.* **2012**, *9*, 585.
[7] H. W. Lee, G. J. Kim, J. M. Kim, J. K. Park, J. K. Lee, G. C. Kim, *J. Endod.* **2009**, *35*, 587.
[8] M. Marschewski, J. Hirschberg, T. Omairi, W. Viol, S. Emmert, W. Maus-Friedrichs, *Exp. Dermatol.* **2012**, *21*, 921.
[9] S. U. Kalghatgi, G. Fridman, M. Cooper, G. Nagaraj, M. Peddinghaus, M. Balasubramanian, V. N. Vasilets, A. F. Gutsol, A. Fridman, G. Friedman, *IEEE Trans. Plasma Sci.* **2007**, *35*, 1559.
[10] H. M. Joh, S. J. Kim, T. H. Chung, S. H. Leem, *Appl. Phys. Lett.* **2012**, *101*, 053703.
[11] N. Barekzi, M. Laroussi, *J. Phys. D: Appl. Phys.* **2012**, *45*, 422002.
[12] N. K. Kaushik, Y. H. Kim, Y. G. Han, E. H. Choi, *Curr. Appl. Phys.* **2013**, *13*, 614.
[13] S. Zhao, Z. Xiong, X. Mao, D. Meng, Q. Lei, Y. Li, P. Deng, M. Chen, M. Tu, X. Lu, G. Yang, G. He, *PLoS ONE* **2013**, *8*, e73665.
[14] G. Fridman, A. Shereshevsky, M. J. Jost, A. D. Brooks, A. Fridman, A. Gutsol, V. Vasilets, G. Friedman, *Plasma Chem. Plasma Process.* **2007**, *27*, 163.
[15] C.-H. Kim, J. H. Bahn, S.-H. Lee, G.-Y. Kim, S.-I. Jun, K. Lee, S. J. Baek, *J. Biotechnol.* **2010**, *150*, 530.
[16] J. Schlegel, J. Köritzer, V. Boxhammer, *Clin. Plasma Med.* **2013**, *1*, 2.
[17] M. Leduc, D. Guay, S. Coulombe, R. L. Leask, *Plasma Process. Polym.* **2010**, *7*, 899.
[18] J. K. Lee, M. S. Kim, J. H. Byun, K. T. Kim, G. C. Kim, G. Y. Park, *Jpn. J. Appl. Phys.* **2011**, *50*, 08JF01.
[19] S. Kalghatgi, C. M. Kelly, E. Cerchar, B. Torabi, O. Alekseev, A. Fridman, G. Friedman, J. A. Clifford, *PLoS ONE* **2011**, *6*, e16270.
[20] H. J. Ahn, K. Il Kim, G. Kim, E. Moon, S. S. Yang, J.-S. Lee, *PLoS ONE* **2011**, *6*, e28154.
[21] X. Yan, Z. Xiong, F. Zou, S. Zhao, X. Lu, G. Yang, G. He, K. Ostrikov, *Plasma Process. Polym.* **2012**, *9*, 59.
[22] G. Fridman, G. Friedman, A. Gutsol, A. B. Shekhter, V. N. Vasilets, A. Fridman, *Plasma Process. Polym.* **2008**, *5*, 503.
[23] J.-W. Lackmann, S. Scheider, E. Edengeiser, F. Jarzina, S. Brinckmann, E. Steinborn, M. Havenith, J. Benedikt, J. E. Bandow, *J. R. Soc. Interface* **2013**, *10*, 20130591.

[24] E. A. J. Bartis, D. B. Graves, J. Seog, G. S. Oehrlein, *J. Phys. D: Appl. Phys.* **2013**, *46*, 312002.
[25] T.-Y. Chung, N. Ning, J.-W. Chu, D. B. Graves, E. Bartis, S. Joonil, et al., *Plasma Process. Polym.* **2013**, *10*, 167.
[26] E. A. J. Bartis, C. Barrett, T.-Y. Chung, N. Ning, J.-W. Chu, D. B. Graves, J. Seog, G. S. Oehrlein, *J. Phys. D: Appl. Phys.* **2014**, *47*, 045202.
[27] E. C. Neyts, M. Yusupov, C. C. Verlackt, A. Bogaerts, *J. Phys. D: Appl. Phys.* **2014**, *47*, 293001.
[28] M. Orazov, Y. Sakiyama, D. B. Graves, *J. Phys. D: Appl. Phys.* **2012**, *45*, 445201.
[29] C. Chen, D. X. Liu, Z. C. Liu, A. J. Yang, H. L. Chen, G. Shama, M. G. Kong, *Plasma Chem. Plasma Process.* **2014**, *34*, 403.
[30] N. Y. Babaeva, M. J. Kushner, *J. Phys. D: Appl. Phys.* **2010**, *43*, 185206.
[31] N. Y. Babaeva, N. Ning, D. B. Graves, M. J. Kushner, *J. Phys. D: Appl. Phys.* **2012**, *45*, 115203.
[32] N. Y. Babaeva, M. J. Kushner, *J. Phys. D: Appl. Phys.* **2013**, *46*, 025401.
[33] C. J. Mundy, M. E. Colvin, A. A. Quong, *J. Phys. Chem. A* **2002**, *106*, 10063.
[34] Y. Wu, C. J. Mundy, M. E. Colvin, R. Car, *J. Phys. Chem. A* **2004**, *108*, 2922.
[35] R. M. Abolfath, D. J. Carlson, Z. J. Chen, R. Nath, *Phys. Med. Biol.* **2013**, *58*, 7143.
[36] D. P. Tieleman, H. Leontiadou, A. E. Mark, S.-J. Marrink, *J. Am. Chem. Soc.* **2003**, *125*, 6382.
[37] A. A. Gurtovenko, I. Vattulainen, *J. Am. Chem. Soc.* **2005**, *127*, 17570.
[38] R. M. Abolfath, A. C. van Duin, T. Brabec, *J. Phys. Chem. A* **2011**, *115*, 11045.
[39] M. Yusupov, E. C. Neyts, U. Khalilov, R. Snoeckx, A. C. T. van Duin, A. Bogaerts, *New J. Phys.* **2012**, *14*, 093043.
[40] M. Yusupov, A. Bogaerts, S. Huygh, R. Snoeckx, A. C. T. van Duin, E. C. Neyts, *J. Phys. Chem. C* **2013**, *117*, 5993.
[41] M. Yusupov, E. C. Neyts, C. C. Verlackt, U. Khalilov, A. C. T. van Duin, A. Bogaerts, *Plasma Process. Polym.* DOI 10.1002/ppap.201400064.
[42] J. Van der Paal, S. Aernouts, A. C. T. van Duin, E. C. Neyts, A. Bogaerts, *J. Phys. D: Appl. Phys.* **2013**, *46*, 395201.
[43] M. Yusupov, E. C. Neyts, P. Simon, G. Berdiyorov, R. Snoeckx, A. C. T. van Duin, A. Bogaerts, *J. Phys. D: Appl. Phys.* **2014**, *47*, 025205.
[44] C. Van Duin, S. Dasgupta, F. Lorant, W. A. Goddard, *J. Phys. Chem. A* **2001**, *105*, 9396.
[45] O. Rahaman, A. C. van Duin, W. A. Goddard, III, D. J. Doren, *J. Phys. Chem. B* **2010**, *115*, 249.
[46] W. Vollmer, S. J. Seligman, *Trends Microbiol.* **2010**, *18*, 59.
[47] W. Vollmer, D. Blanot, M. A. de Pedro, *FEMS Microbiol. Rev.* **2008**, *32*, 149.
[48] N. Bai, P. Sun, H. Zhou, H. Wu, R. Wang, F. Liu, W. Zhu, J. L. Lopez, J. Zhang, J. Fang, *Plasma Process. Polym.* **2011**, *8*, 424.
[49] K. Oehmigen, M. Hähnel, R. Brandenburg, C. Wilke, K. D. Weltmann, T. von Woedtke, *Plasma Process. Polym.* **2010**, *7*, 250.
[50] M. Hähnel, T. von Woedtke, K.-D. Weltmann, *Plasma Process. Polym.* **2010**, *7*, 244.
[51] X. Lu, T. Ye, Y. Cao, Z. Sun, Q. Xiong, Z. Tang, Z. Xiong, J. Hu, Z. Jiang, Y. Pan, *J. Appl. Phys.* **2008**, *104*, 053309.
[52] S. Ikawa, K. Kitano, S. Hamaguchi, *Plasma Process. Polym.* **2010**, *7*, 33.
[53] C. Erridge, E. Bennett-Guerrero, I. R. Poxton, *Microbes Infection* **2002**, *4*, 837.
[54] U. Zahringer, Y. A. Knirel, B. Lindner, J. H. Helbig, A. Sonesson, R. Marre, E. T. Rietschel, *Prog. Clin. Biol. Res.* **1994**, *392*, 113.
[55] J. M. Jungersted, L. I. Hellgren, G. B. E. Jemec, T. Agner, *Contact Dermititis* **2008**, *58*, 255.
[56] J. Ishikawa, H. Narita, N. Kondo, M. Hotta, Y. Takagi, Y. Masukawa, T. Kitahara, Y. Takema, S. Koyano, S. Yamazaki, A. Hatamochi, *J. Investigat. Dermatol.* **2010**, *130*, 2511.
[57] O. Lademann, H. Richter, M. C. Meinke, A. Patzelt, A. Kramer, P. Hinz, K.-D. Weltmann, B. Hartmann, S. Koch, *Exp. Dermatol.* **2011**, *20*, 488.
[58] A. Voter, F. Montalenti, T. Germann, *Annu. Rev. Mater. Res.* **2002**, *32*, 321.
[59] E. Neyts, B. J. Thijsse, M. J. Mees, K. M. Bal, G. Pourtois, *J. Chem. Theory Comput.* **2012**, *8*, 1865.
[60] M. Mees, G. Pourtois, E. Neyts, B. Thijsse, A. Stesmans, *Phys. Rev. B* **2012**, *85*, 134301.
[61] E. C. Neyts, A. Bogaerts, *Theor. Chem. Accounts* **2013**, *132*, 1320.
[62] E. Neyts, Y. Shibuta, A. van Duin, A. Bogaerts, *ACS Nano* **2010**, *4*, 6665.
[63] E. Neyts, A. van Duin, A. Bogaerts, *J. Am. Chem. Soc.* **2011**, *133*, 17225.
[64] M. W. L. Teng, J. B. Swann, C. M. Koebel, R. D. Schreiber, M. J. Smyth, *J. Leuk. Biol.* **2008**, *84*, 988.
[65] R. Kim, M. Emi, K. Tanabe, *Immunology* **2007**, *121*, 1.
[66] D. Hanahan, R. Weinberg, *Cell* **2011**, *144*, 646.
[67] V. Miller, *Antineoplastic Effect of Nonthermal Plasma*, Oral presentation at the "1st International Workshop on Plasmas for Cancer Treatment," March 25–26, 2014, Washington DC, USA.

  DOI: 10.1002/ppap.201400084